A fast adaptive power scheme based on temperature and convergence value for optimal hyperthermia treatment

Huang-Wen Huang[a], Chihng-Tsung Liauh[b], Cheng-Ying Chou[c], Tzu-Ching Shih[d], and Win-Li Lin[e*]

[a]Department of Innovative Information and Technology, Division of Software Engineering, Langyang Campus, Tamkang University, Taiwan.
[b] Department of Mechanical Engineering, Kun-Shan University, Tainan, Taiwan
[c]Department of Bio-Industrial Mechatronics Engineering, National Taiwan University, Taipei, Taiwan
[d]Department of Biomedical Imaging and Radiological Science, China Medical University, Taichung, Taiwan
[e] Institute of Biomedical Engineering, College of Medicine and College of Engineering, National Taiwan University, Taipei, Taiwan

*Correspondence to:

Win-Li Lin, Ph.D.

Institute of Biomedical Engineering,

College of Medicine and College of Engineering,

National Taiwan University

No. 1, Sec. 1, Jen-Ai Road, Taipei, Taiwan

Phone: 886-2-2312-3456 ext. 81445; Fax: 886-2-2394-0049

E-mail: winli@ntu.edu.tw

Abstract

To elevate tissue temperature to therapeutic level (i.e. in the range of 41-45 ℃) fast with optimal power deposition during hyperthermia treatment planning (HTP) is a key treatment processing step. This can facilitate proper management of thermal dose distribution in the treated volume. Traditionally we have treated the tumor volume, without considering possible existing thermally significant vessels, using a simple 1^{st}-order temperature-based adaptive power scheme to determine optimal power deposition distributions. The objectives of this study were to reveal the difficulty of that approach and propose a new fast scheme that could improve upon and substitute for the traditional temperature-based adaptive power scheme.

In this study, we presented a new three-coefficient-and-two-SCV 5^{th}-order temperature-based adaptive power scheme to resolve the induced large blood vessel problem in 3-D temperature distribution and introduced a new parameter, SCV (Sentinel Convergence Value), to handle interior scheme shift.

Results showed the traditional power scheme was sufficient to apply during the optimization process, when the process to obtain optimal absorbed power deposition involves thermal diffusion (i.e. conduction) process only. However the addition of thermal convection by large blood vessel existing in the tumor volume indicated the cooling effect that was the cause for impediment of optimization. Secondly, the new

improved scheme showed its robustness in reducing number of iterations.

This paper addresses a procedure to speed up the optimization process using SCV as a scheme-shift, although the tumor volume consisted of only one thermally significant blood vessel. A new, improved three-coefficient-and-two-SCV 5^{th}-order temperature-based adaptive power scheme has shown its robustness to fast-approach optimal temperature distribution or power density distribution with high precision in the tumor volume when considering the existence of thermally significant blood vessel. Optimally, we are able to effectively calculate the absorbed power density distribution of 3-D biological tissues with a complicating vasculature [1] in the volume.

1. Introduction

Hyperthermia, i.e. elevating temperatures of the tumor to the range of 41-45℃, is used as a modality adjuvant to radiotherapy or chemotherapy in the various cancer treatment types. It has greatly benefited from the development of hyperthermia treatment planning (HTP) [2]. The planning simulates, either simultaneously or beforehand, the heating process and is a valuable component in monitoring the treatment. However, uncertainties exist during computer simulation; recently Greef et al [3] showed the impact of tissue perfusion uncertainty, which is one of many uncertainties, during optimization in hyperthermia treatment planning. They also referred to another significant impact on optimization methods when considering large blood vessels and suggested temperature-based optimization is superior to specific absorption rate (SAR)-based optimization.

In locoregional hyperthermia, in case of application to deep-seated tumors, heating is generally applied using phase-array systems such as high-intensity focused ultrasound (HIFU). The amplitude and phase of every applicator transducer are important parameters to be tuned, thus, to optimize the power density distribution or temperature distribution [4-5]. Kolios et al [6] used HIFU in treatments and showed blood flow cooling of different vessel sizes. Through simulating the heating process, the parameters are determined [7], and the process is a valuable component with

which to monitor treatment. Another type of optimization with constraints on both tumor and normal tissues, such as the complaint-adaptive power density optimization, it was used as a tool for HTP-guided steering in deep hyperthermia treatment [8]. Fast response from the computer was a must.

Traditionally, optimal power deposition patterns for ideal hyperthermia treatment were rather simple: having uniform power deposited in the treated tumor volume. The thermal model in simulation was based on Pennes bio-heat transfer equation (PBHTE) [9]. In addition to blood perfusion (i.e. energy removal term), thermal conduction was the only heat transfer mode considered in the process. The optimization process to determine system coefficients or parameters was rather simple with respect to temperature distribution.

As to considering a thermally significant blood vessel inside or surrounding the deep-treated tumor volume, the whole optimization process may become inapplicable or require irrational iterative computational time. The impact of thermally significant blood vessels has been well recognized since 1980. PBHTE assumed blood could carry heat out and mix with warmer tissue temperatures, and Pennes [10] started the cooling effect by proposing a blood perfusion term in the mathematical formulation. Pennes equation is an approximation to the temperature field without considering impact of large blood vessels. Chen and Holmes [11] investigated

micro-vascular contributions in tissue heat transfer. They presented important properties of vascular compartments. In 1980, Chato [12] investigated heat transfer of blood vessels and indicated that large arteries impacted significantly on surrounding tissue temperatures. Continued from Chato's work, during the 1990s, Huang [13] used a 3-D tissue and blood vessel model to numerically investigate impacts of large blood vessels on hyperthermia cancer treatments, and Huang et al [14] developed analytical solutions of PBHTE with a blood vessel, by neglecting axial conduction effect. Bash [15] presented heat transport by countercurrent blood vessels in the living tissues. Crezee and Lagendijk [16-17] verified experimentally temperature profiles around large artificial vessels in the perfused tissues. Rawnsley et al [18] illustrated the experimental blood temperature data measured in the thighs of anesthetized greyhound dogs under hyperthermic conditions heated by scanned focused ultrasound.

To obtain optimal temperature distribution or power density distribution on a deep-seated tumor volume with inclusion of a thermally significant blood vessel becomes a rather complicated case since both tissue and blood temperatures are significant, and convective cooling effect introduced by the vessel also needs to be taken into consideration. Thus the aim of this paper is to illustrate the difficulty of optimization via temperature-based adaptive power scheme and propose a new,

improved scheme to fast obtain optimal solutions when considering thermally significant blood vessel. In this study, one of our goals was aiming to effectively calculate optimal absorbed power density (PD) distribution in the 3-D vascular system [19-20] (consisting of both tissue and vessel models).

2. Methods

2.1 Formulation of the problem

To present our studies, we used a thermally significant blood vessel passing through a tumor region at the center. The tumor volume was a one-centimeter cube located in the center of the domain. The domain of control volume in the study was 4-cm (H) by 4-cm (W) by 4-cm (L), for it sufficiently described the temperature distributions around the tumor. The geometric model illustrates a thermally significant blood vessel passing through a treated tumor region at the center, with blood moving upward as shown in Figure 1(a). A projection view on X-Z plane of Figure 1(a) with a thermally significant blood vessel entering the treated region is shown in Figure 1(b). The information on significant blood vessel sizes and average mass flow rates are shown in Table 1 [6].

2.2 Mathematical and numerical modelings

Considering a thermally significant blood vessel, blood temperature needs to be calculated. Therefore, combined tissue and blood vessel models were used in the study. The tissue temperature is described by Pennes bio-heat transfer equation. That is,

$$\nabla\bullet(k\nabla T(x,y,z))-\dot{w}_b c_b(T(x,y,z)-T_a)+q_s=0 \qquad (1)$$

where k, c_b, $\dot{w}_b$, and q_s are the thermal conductivity of soft tissue, specific heat of blood, blood perfusion rate and absorbed thermal power density (which is identical to P_n in Equation (6)), respectively. $\bigtriangledown$ is the differential operator. Conduction occurs in all three directions (x, y and z) in the tissue matrix, and the outer control volume surface is held at a constant reference temperature (i.e. identical to the inlet artery temperature).

The convective energy equation is solved for the blood vessel model. That is,

$$m_{bi}c_b\frac{\partial T_b(x,y,z)}{\partial x_i}=Nu\cdot k_b\pi(T_w(x,y,z)-T_b(x,y,z))+q_s\pi R_{bv}^2 \qquad (2)$$

where m_{bi} is the blood mass flow rate at the vessel segments along x_i. x_i is the coordinate axis, which is x, y or z axis. The vasculature consists of straight vessel segments. Nu, k_b, R_{bv} and T_w are the Nusselt number, thermal conductivity in blood, radius of blood vessel and blood vessel wall temperature. We assumed an average uniform velocity profile of blood fluid in vessel, and fully developed flow, as studies had shown insignificant difference when comparing results from those of using non-uniform profile in vessel. The vessel heat transfer coefficient was calculated

using a constant Nusselt number, which was 4.0, as studies [13] indicated there was no significant difference in the range of ±10% of 4.0.

The numerical scheme used to calculate the temperatures was a black and red vectorization finite difference SOR method with upwind differencing used for the vessels. The numerical details are described by Huang [13]. The property values used in treated tumorous and non-treated normal tissues were k = 0.5 W m^{-1}℃$^{-1}$, c = c_b = 4000 J kg^{-1}℃$^{-1}$ and ρ = 1000 kg m^{-3}. For blood, k_b is identical to k. In this study, a finite difference nodal spacing of 1 mm was used. The boundary temperature was set to 37℃ at the outer control volume surfaces. Inlet temperatures of the vessel to the control volume were also set to 37℃.

2.3 Proposed adaptive power optimization scheme

An adaptive optimization scheme was employed to find optimal PD distribution in the treated tumor region during hyperthermia treatment. The optimal PD was reached as tissue temperatures were close to ideal temperatures with respect to CV, through calculation of mathematical models of tissue and blood vessel described in Sec. 2.2. The flow chart of the adaptive scheme, a finer-resolution optimization scheme, to reach ideal temperature in the tumor volume is shown in Figure 2. The

adaptive absorbed power density scheme based on temperature and convergence value (CV) is,

if (CV > **1st SENTINEL CV**) then

$$P_n(x,y,z)=P_{n-1}(x,y,z)+coef1*(T_{ideal}(x,y,z)-T(x,y,z)) \quad (3)$$

else if (CV > **2nd SENTINEL CV**) then

$$P_n(x,y,z)=P_{n-1}(x,y,z)+coef3*(T_{ideal}(x,y,z)-T(x,y,z))^3 \quad (4)$$

else

$$P_n(x,y,z)=P_{n-1}(x,y,z)+coef5*(T_{ideal}(x,y,z)-T(x,y,z))^5 \quad (5)$$

end if

where *P* is absorbed power density (Wm^{-3}) , n is the iteration number, T_{ideal} is ideal temperature and one of important values, sentinel CV (SCV), introduced above is defined as a value which makes adaptive power schemes shift to fast approach terminal (or desired) CV with less iteration. The above scheme lists three coefficients (coef1, coef3 and coef5), two SCVs and 5^{th}-order temperature-based scheme. The coefficients and SCVs will be determined and described in the following Results section. Depending on required precision (i.e. CV), the scheme shifts (i.e. based on SCV) to a different order of temperature-based scheme.

From Figure 3, the optimization for the case of the tumor volume having a 0.2-mm diameter vessel inside, it appeared that insignificant more iterations required to reach CV (=0.05 or 5%) than the case of the tumor without vessel inside. However, the treated tumor volume having 0.8-mm vessel inside increased at least 13 times in

iteration than that without thermally significant vessel inside to reach CV (=0.05 or 5%). It can be expected that more iterations will be required if higher accuracy (such as 2.5% of convergence criterion) of results or higher mass flow rate of blood vessel is needed. This situation required significant time to process adaptive iterations, which was inefficient.

There are two important background factors when calculating temperature distribution using a system of finite difference equations dealing with thermal transport phenomena (conduction and convection) in this study. The first is the initial temperatures are uniform 37 ℃ in the treated tumor volume. This made adaptive temperature-based power increment increase gradually, as well as for temperature distributions. The second is the cooling effect by the blood vessel. Particularly the impinging point of blood vessel on treated tumor volume was the most difficult region to reach ideal temperature. Hence, the amplification of temperature difference (i.e. between ideal and calculated temperatures) near high thermal gradient region would speed up iterative results and we proposed improved schemes.

The traditional scheme was the 1^{st}-order temperature-based adaptive absorbed power density scheme, which was identical to the one published by Huang et al [1], and the scheme was employed to calculate temperature distributions on biological tissues without considering impact of thermally significant blood vessels. It was the

following:

$$P_{n+1}(x,y,z) = P_n(x,y,z) + \Delta P(x,y,z) \quad (6)$$

$$\Delta P(x,y,z) = Coef * \Delta T(x,y,z) \quad (7)$$

$$\Delta T(x,y,z) = T_{ideal} - T(x,y,z) \quad (8)$$

where P is absorbed power density (Wm^{-3}), which is a function of space, *Coef* is 10,000 (i.e. coef1 in the proposed scheme), n is the iteration number and ΔT is the difference between ideal temperature and calculated temperature. The *Coef* has been tried with different values, and was chosen based on smooth convergence rate (without considering optimal solutions at low CV, which value is described in Eqn. (9), and higher blood flow rate). The ideal temperature in the scheme stands for 43℃ in the treated tumor region in this study.

Conditional statement in the chart, shown in Figure 2, introduced an important adaptive process for the heated tumor volume. That was, the evaluation criterion shown in Equation (9),

$$\frac{\sqrt{\dfrac{\sum_{all\ target\ nodes} ((\Delta T(x,y,z))^2}{total\ number\ of\ target\ nodes}}}{(43-37)\ ^oC} \le convergence\ value\ (CV) \quad (9)$$

Equation 9 showed an important term, the convergence value (CV), which is a

macroscopic parameter correlated to temperature differences at target nodes. Later we introduced a microscopic parameter, dtindex, which described the status of temperature difference at each selected node. When a thermally significant blood vessel ran through the center of a tumor volume, the number of iterations required to reach CV during optimization process, increased as the mass flow rate of blood vessel increased. Figure 3 shows graphs of convergence value (CV) and iterations for several different sizes (i.e. 0.2-mm, 0.6-mm and 0.8-mm diameter) of blood vessel running through the tumor volume, as well as for no vessel inside the tumor. Figure 4 shows (top row) temperature distributions: contours ranging from 37℃ to 43℃ with a step size of 0.5℃, and (bottom row) their corresponding absorbed power density distributions: contours ranging from 2E5 Wm^{-3} to 2E8 Wm^{-3} with a step size of 14E5 Wm^{-3}, in the centric XZ plane, which consists of a thermally significant blood vessel of 0.8, 0.6, 0.2-mm diameter and none from left to right, respectively, within the tumor volume. The CV was 5%.

2.4 A parameter "dtindex": the index of temperature difference between calculated and ideal (or desired) temperatures in the treated volume

A parameter "dtindex" is introduced here to illustrate the temperature difference between calculated and ideal temperatures in the treated volume during optimization

process to reach precision at some convergence value. The "dtindex" is defined as:

$$dtindex = \frac{\left|T_{ideal}(x,y,z) - T(x,y,z)\right|}{6.0} \qquad (10)$$

and it is a function of space. Ideal temperature distribution in the treated volume was assumed uniformly 43℃ in the present study. The divisor of 6 was chosen due to the increment of temperature from initial 37℃ to the ideal 43℃. The absolute of the temperature difference showed the magnitude of distance from the ideal temperature 43℃ to the temperature at the location. The value of "dtindex" is positive and ranged from 0.0 to 1.0 in normal operations (i.e. gradual temperature increments toward ideal temperature). A value near 0.0 means the temperature approaches very close to ideal temperature and if near 1.0 means the temperature moves away from the ideal temperature.

Results

Difficulties of reaching optimal solutions are shown in Figures 3 and 4. To quickly reach ideal therapeutic temperature distribution at a certain CV, the SCVs and adaptive power readjustment scheme coefficients need to be determined. Optimization of SCVs and coefficients used in the proposed schemes shown in Eqns. (3)-(5) are described in the following.

3.1 Setting up the first SCV

As shown in Figure 3, at CV = 0.08, iterative process showed sign of slowdown to reach the target CV (i.e. 0.05). Hence, to reduce iterations and speed up processing, we set up a SCV which makes iterative transition between two distinct temperature-based schemes. In addition, we compared with the traditional simple scheme used in Huang et al [1]. The scheme is described in Eqn. (3) and the coef1 was 10,000.

The first SCV in the new scheme separated the 1^{st}-order temperature-based power readjustment scheme (the traditional one) from the 3^{rd}-order one as described in Eqn. (4). The comparison in Figure 5 shows different SCVs of iterative optimization processes at CV (down up to 0.05) and iteration values for the treated tumor with a 0.8-mm vessel inside. The CV data were selected at every 10 iterations from the

beginning to the end for all Figures 5-8.

The purpose of this step was to find an optimal SCV that could accelerate reaching solution with fewer iterations, with coef1 (in 1^{st}-order scheme) = 10,000 and coef3 (in 3^{rd}-order scheme) = 40,000. The coef1 chosen was to compare with the traditional power readjustment, one-coefficient scheme. Also, the coef3 was chosen due to the ease of reaching an optimal solution with several initial trials. Figure 5 showed different SCVs with the new 3^{rd}-order adaptive optimization scheme (i.e. Eqn. (4)). As highlighted with dark thick line in Figure 5, the first SCV of 0.28 was chosen due to its smallest number of iterations to reach CV of 0.05. Although SCVs of 0.30 and 0.32 also made better results than SCV of 0.28, they showed an early "up-down" perturbation. The cases for SCVs of 0.36 and 0.40 showed increasing sign of oscillating. As shown, for SCV of 0.42, it was a severely diverging situation. Up to this step, the new scheme according to Eqn. (4) used two tuned coefficients to reduce iteration numbers significantly and the first SCV was defined as 0.28.

3.2 Tuning the coefficients for the 3^{rd}-order temperature-based scheme

With fixed coef1 of 10,000, the traditional scheme to be compared, and defined first SCV of 0.28, we further reevaluated the coef3 value. Reconfirmed the value for coef3 and the coef3 of 60,000 was an optimal solution which caused the smallest

number of iterations without severely oscillating. The CV and iteration plot shown in Figure 6 illustrated optimization processes for different coef3 values in the tumor volume with 0.8-mm vessel inside. The terminal CV was 0.04, which value caused iteration to stop. Also, the terminal CV was chosen because of attempting to observe zero absolute value of slope in the graph of CV and iteration plot. Hence, the coef3 was redefined as 60,000, as highlighted with dark thick line in Figure 6. Figure 6 shows the comparison of different coef3 values in the new adaptive optimization scheme (described in Eqn. (4)) after the determination of first SCV. Up to this step, we have considered already optimal solutions in the sense of vertical span (via first SCV) and horizontal span (via coef3) during execution of two-coefficient 3rd-order temperature-based power readjustment scheme, based on the blood flow rate of a 0.8-mm diameter vessel.

3.3 Setting up the second SCV and tuning the coefficients for the 5th-order temperature-based scheme

With the indication of a large vessel size such as 0.8-mm diameter, difficulty occurred as we pursued more accurate solutions (for example, 0.025); they were slow down at CV = 0.04, as shown in Figure 6. Thus we proposed another higher-order scheme to deal with when CV reached 0.04 and below. At this point, we set the

second SCV to 0.04.

Figure 7 shows comparison of different coef5 values in the new 5th-order adaptive optimization scheme (described in Eqn. (5)) with the defined second sentinel CV of 0.04, coef1 value of 10,000 and coef3 value of 60,000. The CV and iteration plot illustrated for the treated tumor volume with 0.8-mm vessel inside and the terminal CV is 0.025, which value caused iterations to stop. Hence, the coef5 was defined as 300,000, as highlighted with dark thick line in Figure 7. It caused less iteration to reach terminal CV.

3.4 Comparison of a new improved three-coefficient scheme and the traditional one-coefficient scheme.

Based on the procedure (described through Sec. 3.1 to Sec. 3.3) to optimize the SCVs and scheme coefficients, we integrated the complete scheme, the 5th-order three-coefficient-two-SCV power readjustment scheme, to be a new improved scheme which could process CV in the range of 0.025 to 1.

Figure 8(a) shows the comparison of traditional one-coefficient power readjustment scheme and a new, improved three-coefficient scheme for a tumor volume having a 0.8-mm diameter thermally significant blood vessel. The terminal CV was 0.025. The required number of iterations for the improved scheme was 233 to

reach terminal CV, and that for the traditional one was approximate 17,200. With cases of lesser and greater blood flow rates for vessels (0.6-mm and 1.0-mm, shown in Figure 8(b) and (c)), the required iterations were 150 and 328 for the new improved scheme and those for the traditional one were 7,050 and 31,317, respectively.

Discussion

4.1 Cooling effect by convection makes optimization difficult

As absorbed power deposition readjustment occurred in the local medium during optimization process, the convection made blood move energy along the path. Thus, it was hard to dissipate absorbed power to surrounding tissue. The cases of no vessel and a 0.2-mm vessel inside the tumor showed almost identical fast speed to reach CV of 0.05, as shown in Figure 3. When size of vessel became larger, such as 0.6-mm and 0.8-mm vessel, an increased in mass flow rate, the numbers of iterations increased approximate 5 and 13 times that for a 0.2-mm diameter vessel case, respectively.

The thermal resistances along vessel path and across vessel wall were not the same. This made the increment of blood temperature change at iteration of absorbed power readjustment small. The other key factor was due to blood temperature at the upstream. As mass flow rate increased, the increment of blood temperature change decreased. Long duration of iteration to raise blood temperature was expected, as shown in Figure 4. The 0.8-mm diameter vessel had longer cooling length at the impinging region on the tumor than the vessels of smaller sizes at CV of 5%.

4.2 dtindex map

Figure 9 shows a dtindex map at various CVs (0.1 (10%), 0.05 (5%) and 0.025

(2.5%)) on the XZ plane having a thermally significant vessel of 0.8-mm diameter at the center. These figures were revealed during adaptive power scheme optimization from CV of 0.1, gradual moving to higher precision, to CV of 0.025. The tissue region, governed by thermal conduction, of those figures showed very small dtindex value and it reached ideal temperatures first. Although four corners' dtindex in the tissue plane were rather higher than their surrounding tissue, comparably, they were still far smaller than the thermal convection region induced by blood vessel.

Figures 9(a) and 9(b) show highest dtindex value at the vessel entrance to the treated tumor due to the cooling impact existing at the impinging location of vessel for CV = 10 % and 5%. However the situation reversed in Figure 9(c) for CV = 2.5 %, the high long dtindex value was located in the middle of vessel. Blood temperatures in the middle of vessel reached over 43℃ due to, in a similar way, slow decrement and accumulation of thermal energy via convection (by the upstream of vessel) and conduction (by surrounding tissue) at the middle of vessel. Although there was not any absorbed power deposition in the middle of blood vessel at CV = 2.5 %, the high dtindex value no longer only existed at the impinging point of blood vessel on the tumor.

4.3 The robustness of the proposed scheme

After determining coefficients and SCVs, a new scheme for the case of a 0.8-mm vessel inside tumor was established. As compared with the old scheme (i.e. one coefficient) with CV = 0.025, it showed significant difference in reducing number of iterations for the improved scheme, as shown in Figure 8(a). Figure 8(b) shows the comparison of two schemes (OLD vs. NEW) for smaller size of vessel (i.e. 0.6-mm) with lower mass flow rate; it revealed the scheme's fast approach to CV of 2.5% as the as the Figure 8(a). On the other hand, we also compared two schemes for larger size of vessel (i.e. 1.0-mm) with increased mass flow rate. The new scheme also showed it's robustness in reducing number of iterations when a thermally significant blood vessel existed in the tumor volume as shown in Figure 8(c).

This demonstrated that our approach to find a new improved temperature-based power scheme was appropriate.

4.4 Oscillation in transition

During scheme-shift process at any SCV, CV oscillation existed in the transition. CV oscillation magnitudes then gradually reduced to zero (i.e. convergence), and iterative optimization continued down to reach target CV, as shown in Figure 8. In case of divergence during iterative optimization, as shown in Figures 5 and 6, the system parameter (scheme coefficient or SCV) was unable to drive the scheme to the

optimal power density distribution under the environment. On the other hand, with the newly determined improved scheme, the change of different environment (or system) would possibly cause the adaptive optimization processes to diverge as well.

Another point to be observed during adaptive process is the absolute value of the slope of CV vs. iteration in the plot. As the value decreased continuously to approach zero during the iterative process, it indicated that adaptive power scheme optimization had slowed its pace. It signaled a possibility that we were dealing with power deposition in blood at this moment.

Our studies suggested, clinically in the HTP, the existence of thermally significant vessel in the treated tumor volume should be identified and handled properly to prevent ineffective or erroneous system response which, therefore, corresponds to unreasonable temperature or power distribution at some local spots.

Conclusion

Thermal convection of thermally significant vessel caused cooling effect on the tumor volume that could significantly impede and slow down adaptive optimization process. The vessel's convection effect appeared clearly as blood flow rate of the vessel increased.

A new, improved three-coefficient-and-two-SCV 5^{th}-order temperature-based adaptive power scheme has shown its robust speed to fast approach optimal temperature distribution or power density distribution with high precision in the tumor volume when considering the existence of a thermally significant blood vessel.

This paper has addressed a procedure to speed up optimization process using SCV as scheme-shift, although the treated tumor volume consisted of only one thermally significant blood vessel. Future work should consider systems of multiple vessels in the volume during adaptive optimization process to reach precision at desired CV.

Reference

[1] H.W. Huang, C.T. Liauh, T.C. Shih, T.L. Horng, W.L. Lin Significance of blood vessels in optimization of absorbed power and temperature distributions during hyperthermia, International Journal of Heat and Mass Transfer 53 (2010) 5651-5662.

[2] J J W Lagendijk, Hyperthermia treatment planning, Phys. Med. Biol. 45 (2000) 61-76.

[3] M. de Greef, H. P. Kok, D. Correia, A. Bel, and J. Crezee, Optimization in hyperthermia treatment planning: The impact of tissue perfusion uncertainty, Medical Physics 37 (9) (2010) 4540-4550.

[4] W.L. Lin, T. C. Liang, J. Y. Yen, H. L. Liu and Y. Y. Chen, Optimization of power deposition, and a heating strategy for external ultrasound thermal therapy, Medical Physics 28 (10) (2001) 2172-2181.

[5] H. S. Tharp and R. B. Roemer, Optimal power deposition with finite-sized, planar hyperthermia applicator arrays, IEEE Trans Biomed Eng. 39 (6) (1992) 569-79.

[6] M. C. Kolios, M. D. Sherar and J. W. Hunt, Blood flow cooling and ultrasonic lesion formation, Med. Phys., 23 (7) (1996) 1287-98.

[7] H P Kok, P M A Van Haaren, J B Van de Kamer, J Wiersma, J D P Van Dijk and J Crezee, High-resolution temperature-based optimization for hyperthermia treatment planning, Physics in Medicine and Biology 50 (2005) 3127-3141.

[8] R A M Canters, M Franckena, J van der Zee and G C Van Rhoon, Complaint-adaptive power density optimization as a tool for HTP-guided steering in deep hyperthermia treatment of pelvic tumors, Physics in Medicine and Biology 53 (2008) 6799-6820.

[9] K.-S. Cheng and R. B. Roemer, Optimal power deposition patterns for ideal high temperature therapy/hyperthermia treatments, Int. J. Hyperthermia 20 (2004), 57-72.

[10] H. H. Pennes, Analysis of tissue and arterial blood temperature in the resting human forearm, J. Appl. Phys. 1 (1948) 93-122.

[11] M. M. Chen and K. R. Holmes, Microvascular contributions in tissue heat transfer, Ann. N.Y. Acad. Sci. 335 **(**1980) 137-150.

[12] J. C. Chato, Heat transfer to blood vessels, ASME J. Biomech. Eng. 110 (1980) 110–18.

[13] H. W. Huang, Simulation of large vessels in hyperthermia therapy, M.S. thesis. University of Arizona, Tucson, AZ, 1992.

[14] H. W. Huang, C. L. Chan and R. B. Roemer, Analytical solutions of Pennes bio-heat transfer equation with a blood vessel, ASME J. Biomech. Eng. 116 **(**1994) 208-12.

[15] J. W. Baish, Heat transport by counter current blood vessels in the presence of an arbitrary temperature gradient, ASME Journal of Biomechanical Engineering 112 (1990) 207-211.

[16] J. Crezee and J. J. W. Lagendijk, Experimental verification of bio-heat transfer theories: measurement of temperature profiles around large artificial vessels in perfused tissues, Phys. of Med. Bio. 35 (1990) 905-23.

[17] J. Crezee and J. J. W. Lagendijk, Temperature uniformity during during hyperthermia: The impact of large vessels, Phys. Med. Biol. **37** (1992) 1321-37.

[18] R. Rawnsley, R. B. Roemer and A. Dutton, The simulation of large vessel effects in experimental hyperthermia, ASME Journal of Biomechanical Engineering 116 **(**1994) 256-62.

[19] H.-W. Huang, T.-C. Shih and C.-T. Liauh, Predicting effects of blood flow rate and size of vessels in a vasculature on hyperthermia treatments using computer simulation, BioMedical Engineering OnLine **9** (2010) 18.

[20] H.-W. Huang, T.-C. Shih, C.-T. Liauh and Tzyy-Leng Horng, Computer simulation of 3-d temperature and power distributions in tissue with a countercurrent blood vessels network during hyperthermia, Journal of Medical and Biological Engineering 29 (5) (2009), 252-258.

Figure Captions

Figure 1. (a) The geometric model illustrates a thermally significant blood vessel passing through a tumor region at the center, with blood moving upward. (b) A projection view on the centric X-Z plane of Figure 1(a) illustrating a thermally significant blood vessel. (0, 0) in X-Z coordinate indicates blood vessel at the boundary entering the control volume.

Figure 2. The flow chart of a finer-resolution adaptive power optimization scheme to reach ideal temperature at the treated region.

Figure 3. Comparison of CV and iteration, using the traditional adaptive 1^{st} -order temperature-based optimization scheme, for the tumor volume without and with a thermally significant blood vessel of different sizes (i.e. 0.2-mm, 0.6-mm and 0.8-mm diameter).

Figure 4. (Top row) temperature distributions and (bottom row) their corresponding absorbed power density distributions in the centric XZ plane, which consists of a thermally significant blood vessel of 0.8, 0.6, 0.2-mm diameter and none from left to right, respectively, within the tumor volume. The CV is 5%. (units in figure, t: ℃

and power: Wm^{-3})

Figure 5. Applied with new adaptive optimization scheme described in Eqn. (4) with different SCVs. The first SCV in the new scheme separated the 1^{st}-oder temperature power readjustment scheme (the traditional one) from the 3^{rd}-order one. The comparison showed CV (down up to 0.05) and iteration for the treated tumor with a 0.8-mm vessel inside. The new scheme used two tuned values (10,000 and 40,000) to reduce iteration numbers significantly and the first SCV was defined as 0.28.

Figure 6. Comparison of different coef3 values in the new adaptive optimization scheme described in Eqn. (4) with defined first SCV of 0.28 and coef1 value of 10,000. The CV vs. iteration plot is for the treated tumor volume with 0.8-mm vessel inside during adaptive optimization process, and the terminal CV is 0.04, which value caused iteration to stop. Hence, the coef3 was defined as 60,000.

Figure 7. Comparison of different coef5 values in the new adaptive optimization scheme described in Eqn. (5) with the defined first SCV of 0.28, second SCV of 0.04, coef1 value of 10,000 and coef3 value of 60,000. The CV vs. iteration plot is for the tumor volume with 0.8-mm vessel inside, and the terminal CV is 0.025, which value

caused iteration to stop. Hence, coef5 was defined as 300,000.

Figure 8. Comparison of traditional one-coefficient power readjustment scheme and new, improved three-coefficient scheme for the tumor volume having different sizes of thermally significant blood vessel: (a) 0.8-mm diameter (b) 0.6-mm diameter and (c) 1.0-mm diameter.

Figure 9. dtindex map on the XZ plane having a thermally significant vessel of 0.8-mm diameter at various CVs. (a) CV = 0.1 (b) CV = 0.05 (c) CV =0.025

Table Captions

Table 1. Significant vessel diameters and average flow rates from Kolios et al [6].

(a)

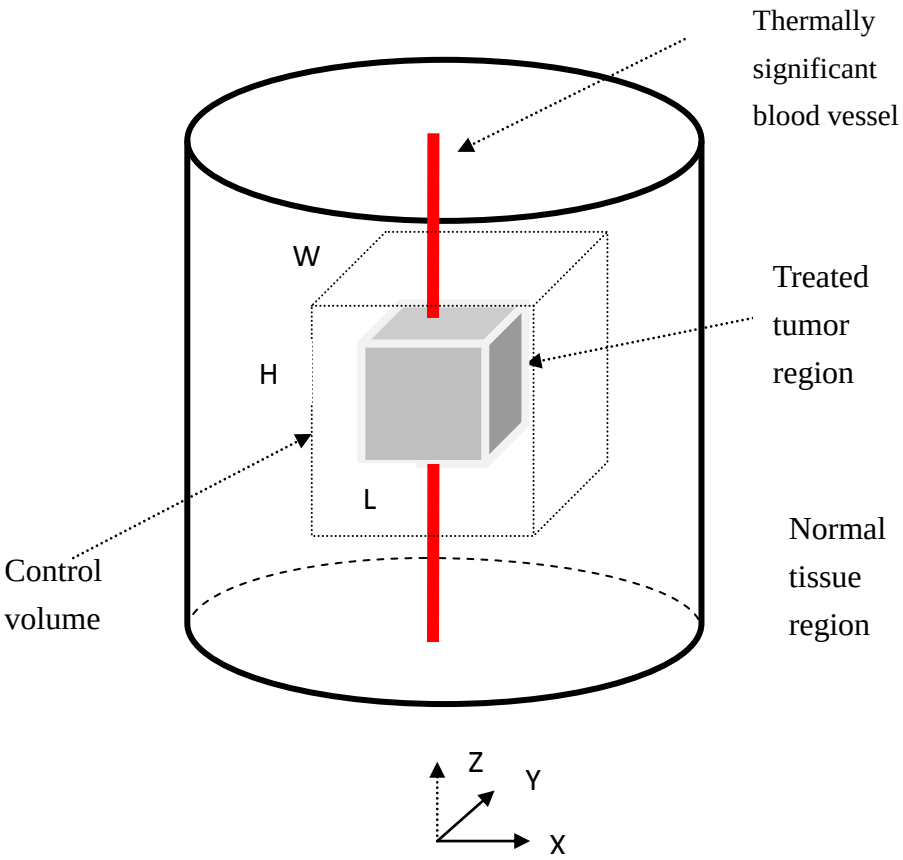
Thermally
significant
blood vessel
W
H
L
Treated
tumor
region
Control
volume
Normal
tissue
region
Z
Y
X

(b)

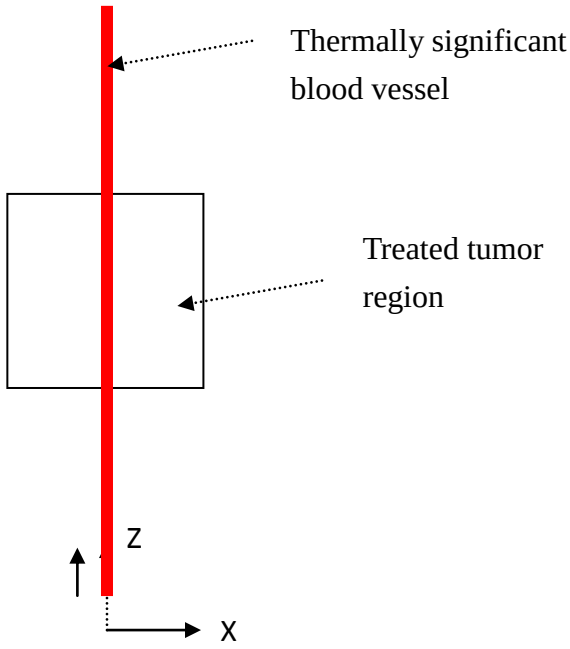
Thermally significant
blood vessel
Treated tumor
region
Z
X

FIG.1

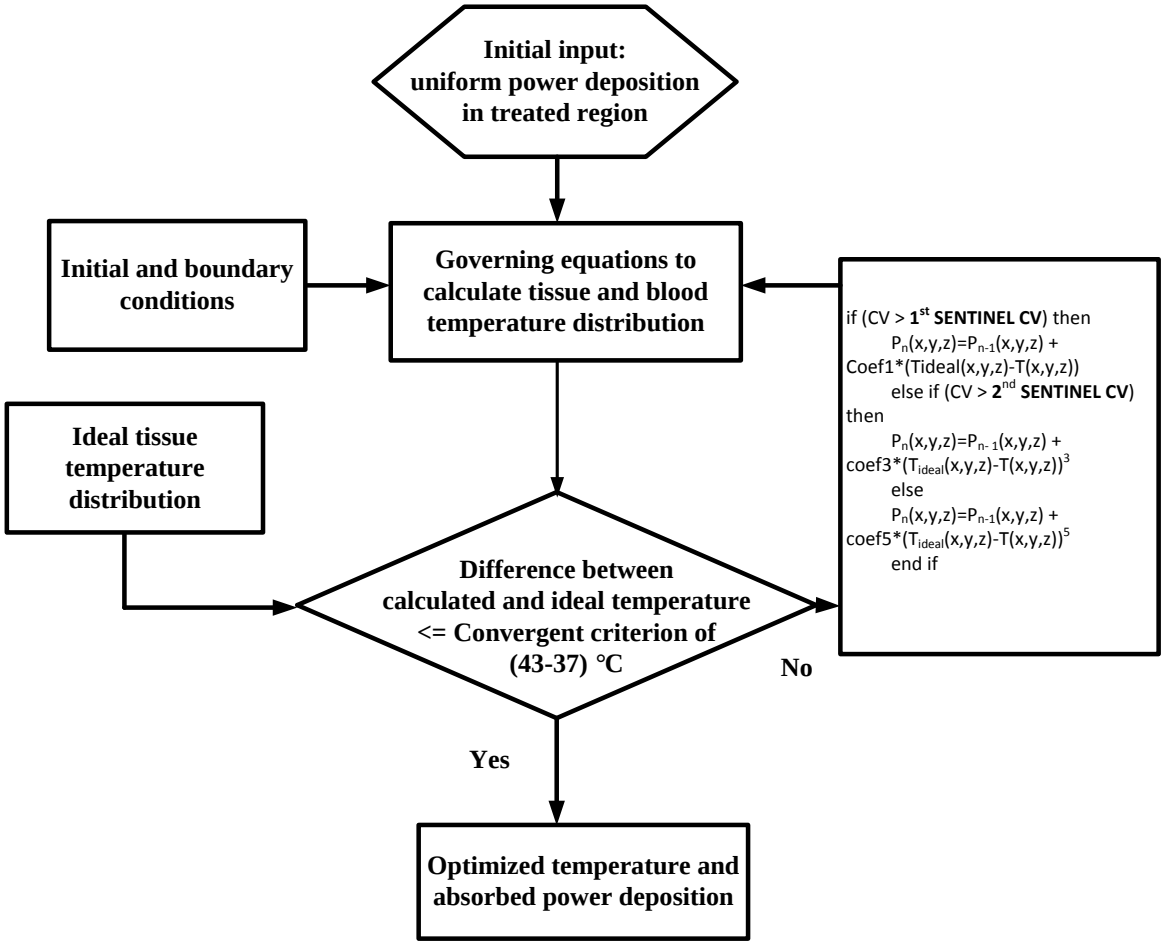
Initial input: uniform power deposition in treated region
Initial and boundary conditions
Governing equations to calculate tissue and blood temperature distribution
Ideal tissue temperature distribution
Difference between calculated and ideal temperature <= Convergent criterion of (43-37) °C
No
Yes
Optimized temperature and absorbed power deposition
if (CV > 1st SENTINEL CV) then
Pn(x,y,z)=Pn-1(x,y,z) + Coef1*(Tideal(x,y,z)-T(x,y,z))
else if (CV > 2nd SENTINEL CV) then
Pn(x,y,z)=Pn-1(x,y,z) + coef3*(Tideal(x,y,z)-T(x,y,z))3
else
Pn(x,y,z)=Pn-1(x,y,z) + coef5*(Tideal(x,y,z)-T(x,y,z))5
end if

FIG. 2

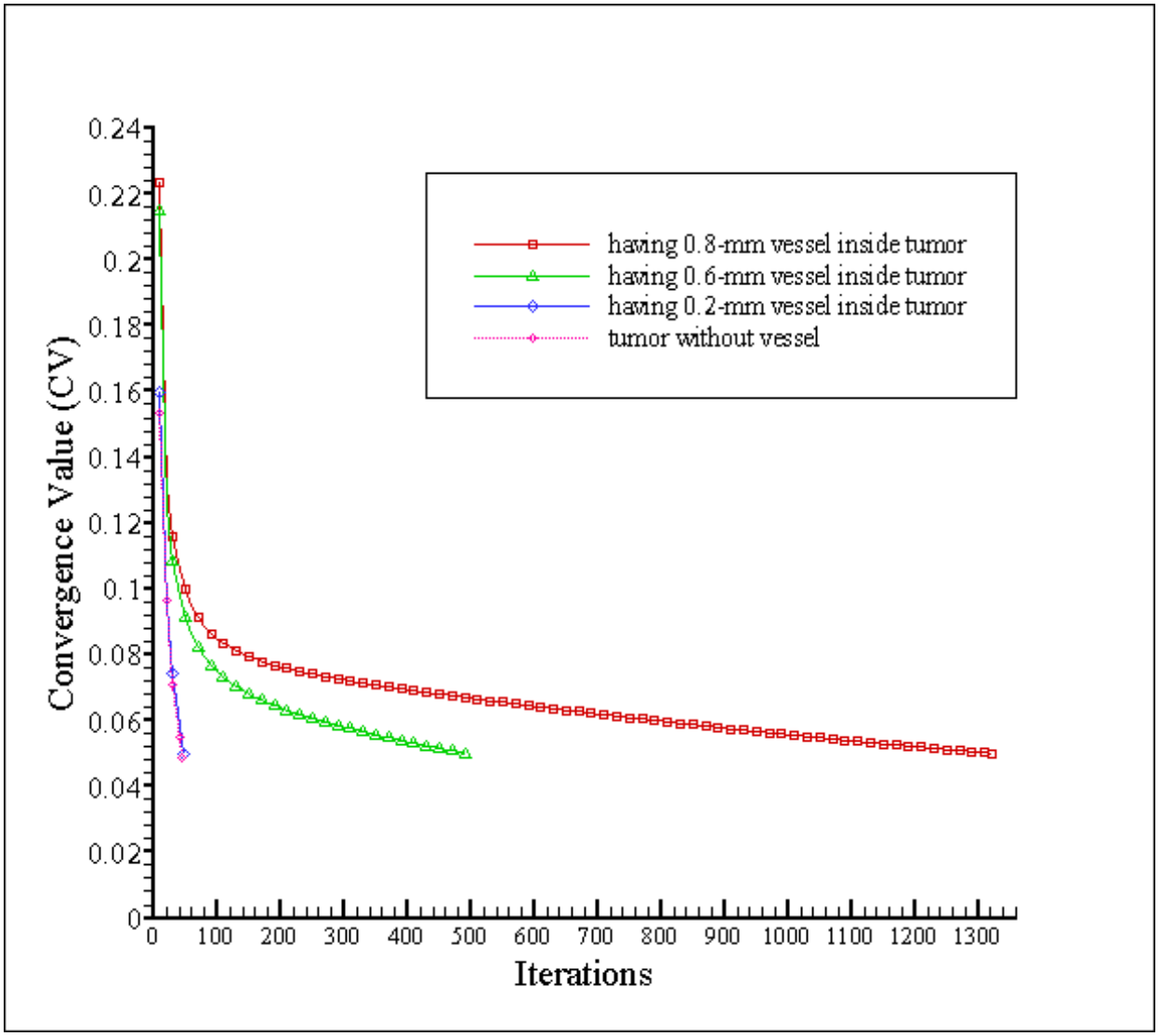
having 0.8-mm vessel inside tumor
having 0.6-mm vessel inside tumor
having 0.2-mm vessel inside tumor
tumor without vessel
Convergence Value (CV)
0.24
0.22
0.2
0.18
0.16
0.14
0.12
0.1
0.08
0.06
0.04
0.02
0
0 100 200 300 400 500 600 700 800 900 1000 1100 1200 1300
Iterations

FIG. 3

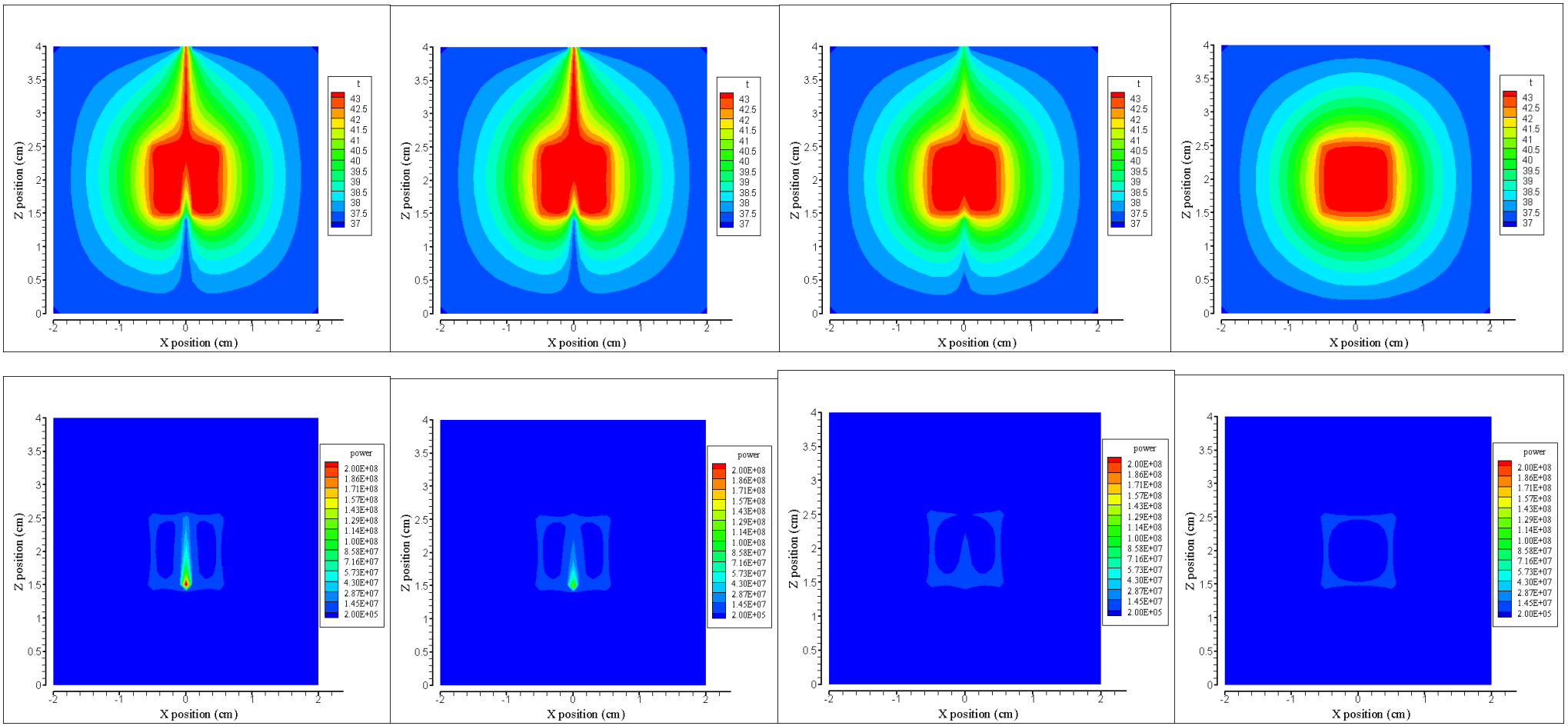
Z position (cm)
X position (cm)
t
43
42.5
42
41.5
41
40.5
40
39.5
39
38.5
38
37.5
37
power
2.00E+08
1.86E+08
1.71E+08
1.57E+08
1.43E+08
1.29E+08
1.14E+08
1.00E+08
8.58E+07
7.16E+07
5.73E+07
4.30E+07
2.87E+07
1.45E+07
2.00E+05

FIG. 4

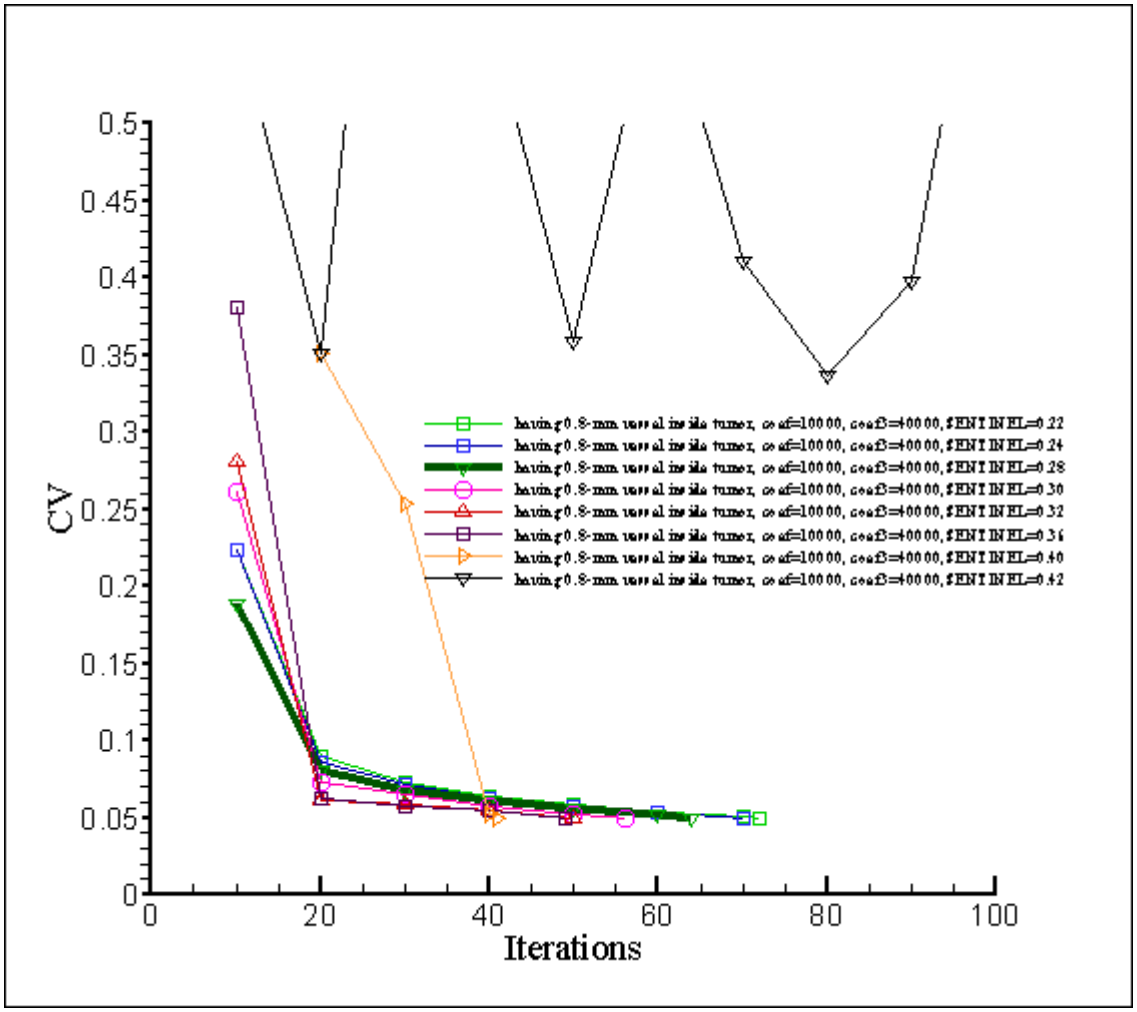
CV
Iterations
0
0.05
0.1
0.15
0.2
0.25
0.3
0.35
0.4
0.45
0.5
0
20
40
60
80
100

FIG. 5

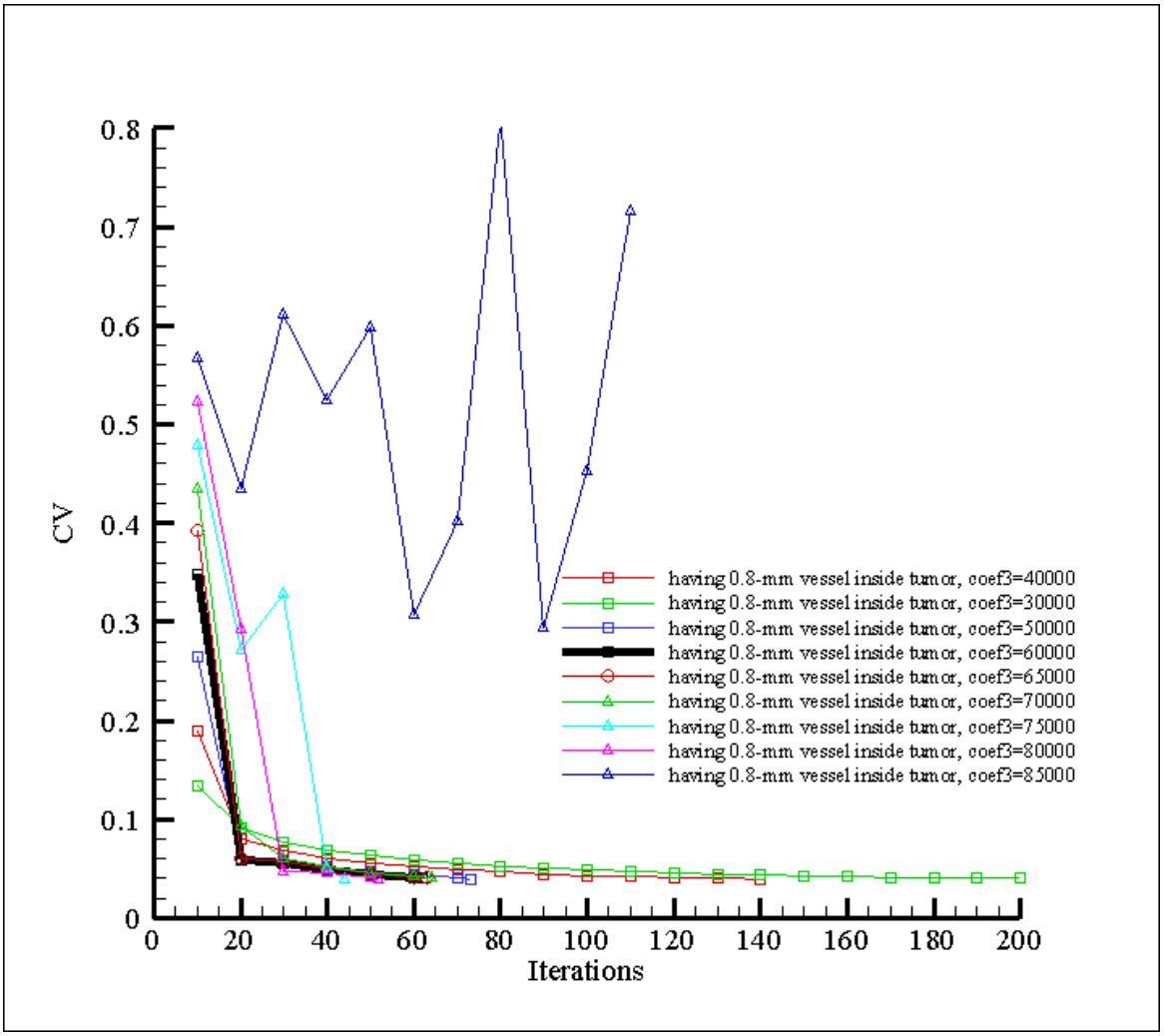
CV
Iterations
0
0.1
0.2
0.3
0.4
0.5
0.6
0.7
0.8
0
20
40
60
80
100
120
140
160
180
200
having 0.8-mm vessel inside tumor, coef3=40000
having 0.8-mm vessel inside tumor, coef3=30000
having 0.8-mm vessel inside tumor, coef3=50000
having 0.8-mm vessel inside tumor, coef3=60000
having 0.8-mm vessel inside tumor, coef3=65000
having 0.8-mm vessel inside tumor, coef3=70000
having 0.8-mm vessel inside tumor, coef3=75000
having 0.8-mm vessel inside tumor, coef3=80000
having 0.8-mm vessel inside tumor, coef3=85000

FIG. 6

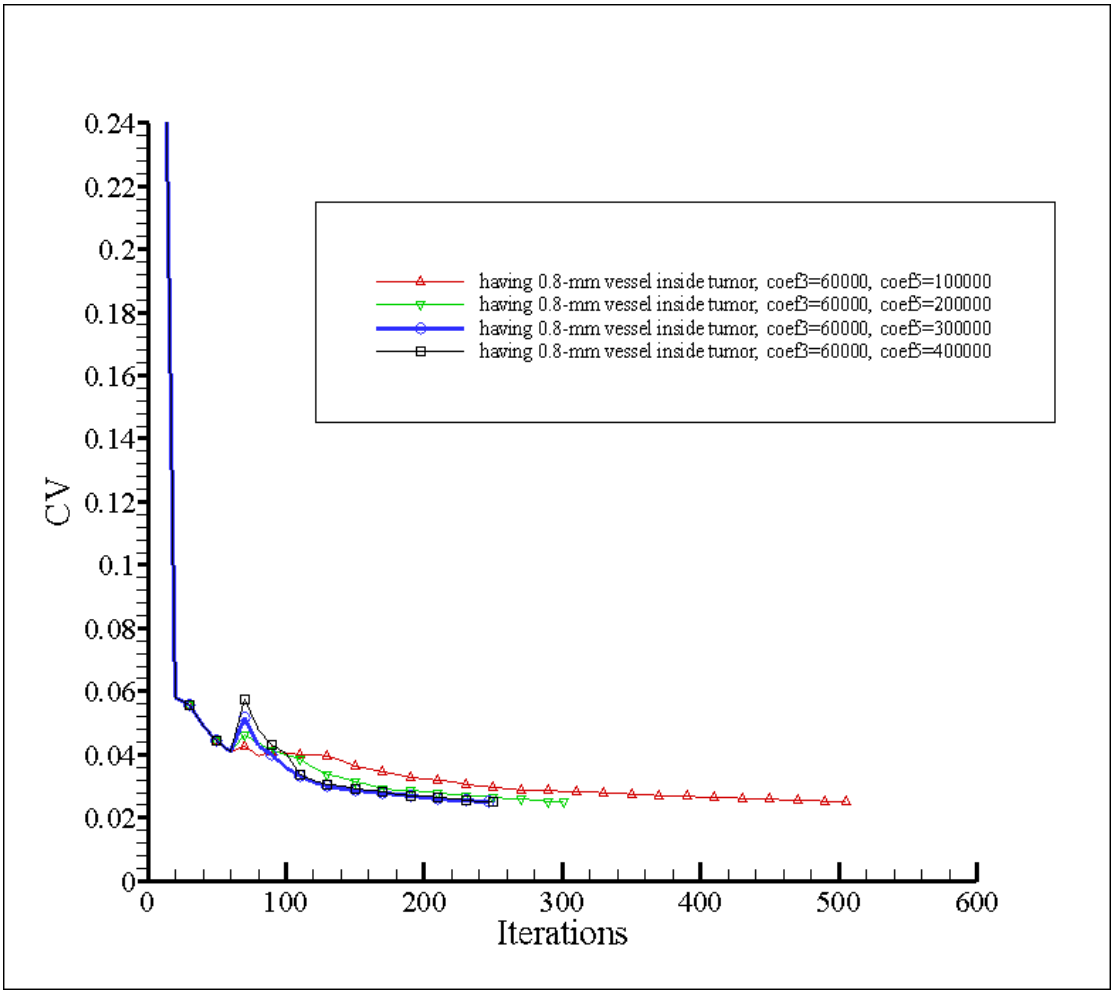
0.24
0.22
0.2
0.18
0.16
0.14
0.12
0.1
0.08
0.06
0.04
0.02
0
CV
0
100
200
300
400
500
600
Iterations
having 0.8-mm vessel inside tumor, coef3=60000, coef5=100000
having 0.8-mm vessel inside tumor, coef3=60000, coef5=200000
having 0.8-mm vessel inside tumor, coef3=60000, coef5=300000
having 0.8-mm vessel inside tumor, coef3=60000, coef5=400000

FIG. 7

(a)

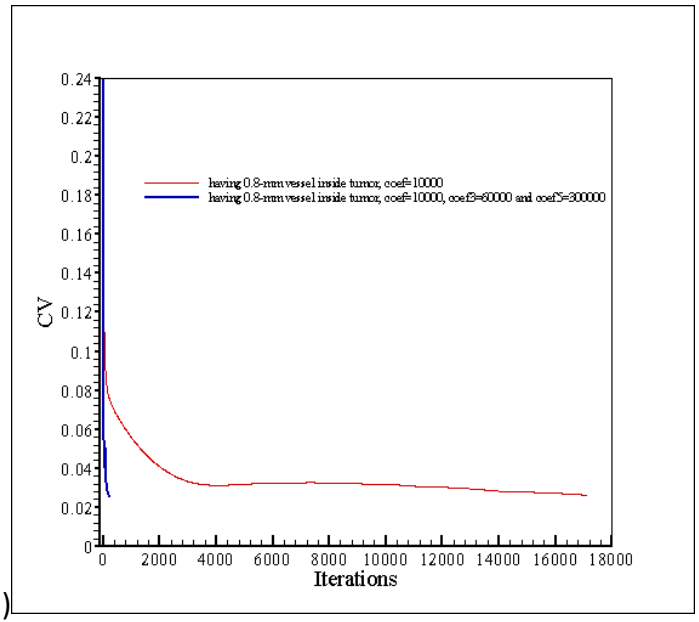
having 0.8-mm vessel inside tumor, coef=10000
having 0.8-mm vessel inside tumor, coef=10000, coef3=60000 and coef5=300000
CV
Iterations

(b)

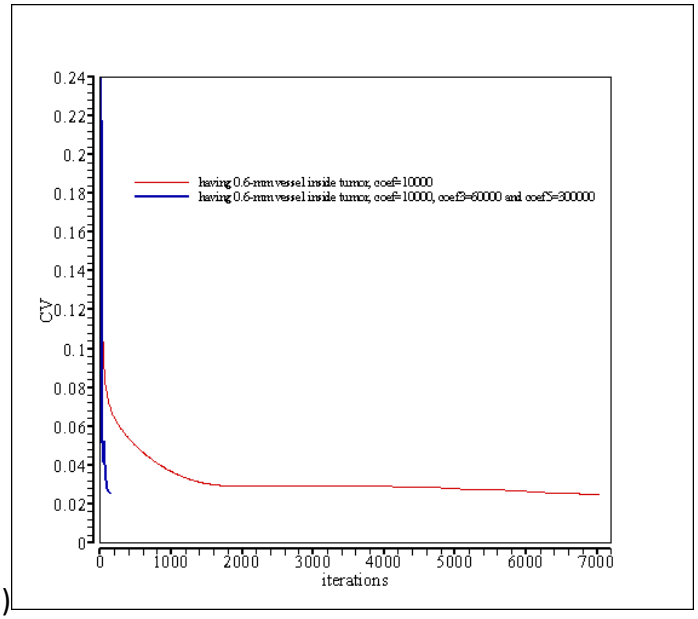
having 0.6-mm vessel inside tumor, coef=10000
having 0.6-mm vessel inside tumor, coef=10000, coef3=60000 and coef5=300000
CV
iterations

(c)

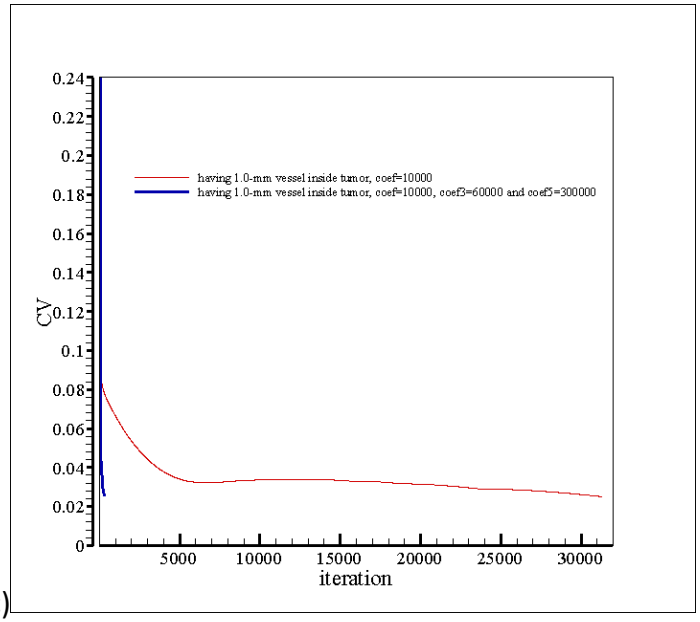
having 1.0-mm vessel inside tumor, coef=10000
having 1.0-mm vessel inside tumor, coef=10000, coef3=60000 and coef5=300000
CV
iteration

FIG. 8

(a)

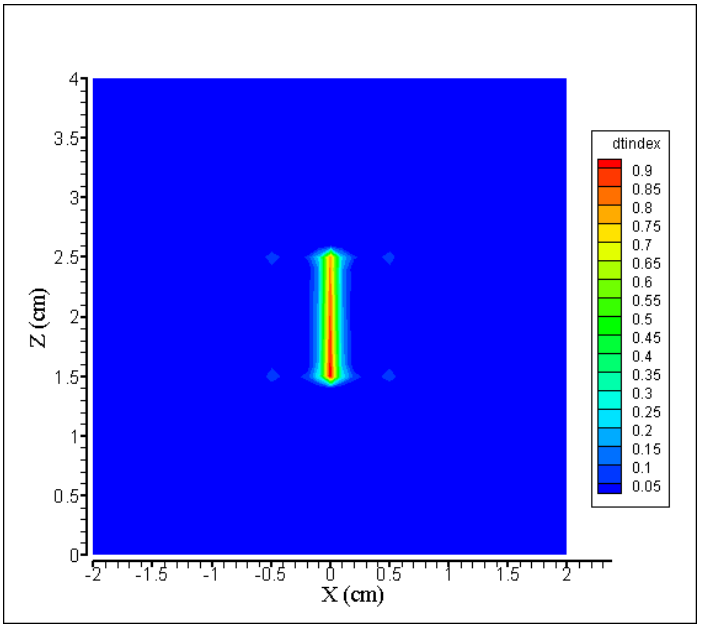
dtindex
0.9
0.85
0.8
0.75
0.7
0.65
0.6
0.55
0.5
0.45
0.4
0.35
0.3
0.25
0.2
0.15
0.1
0.05
Z (cm)
X (cm)

(b)

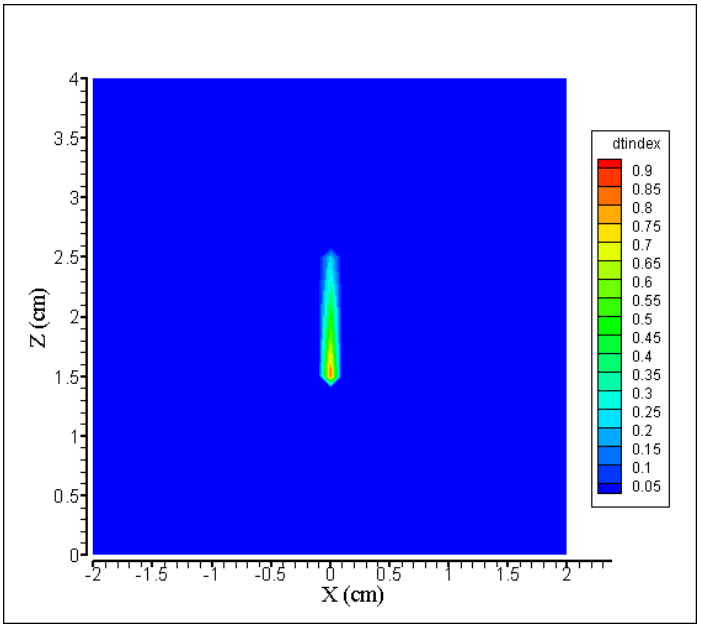
dtindex
0.9
0.85
0.8
0.75
0.7
0.65
0.6
0.55
0.5
0.45
0.4
0.35
0.3
0.25
0.2
0.15
0.1
0.05
Z (cm)
X (cm)

(c)

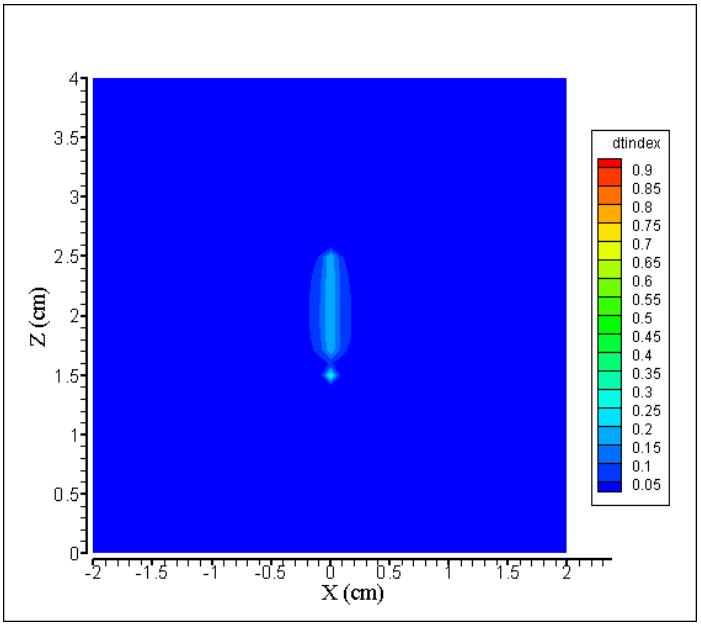
dtindex
0.9
0.85
0.8
0.75
0.7
0.65
0.6
0.55
0.5
0.45
0.4
0.35
0.3
0.25
0.2
0.15
0.1
0.05
Z (cm)
X (cm)

FIG. 9

Table 1.

Blood vessel diameter (mm)	Average velocity (cm/s)
1.4	10.5
1.0	8.0
0.8	7.5
0.6	6.0
0.4	5.5
0.2	3.4